JOURNAL OF APPLIED ELECTROCHEMISTRY 23 (1993) 735–740

Chemical and electrochemical behaviour of nickel ions in the $ZnCl_2$–2NaCl melt at 450° C

D. FERRY†, G. PICARD

Laboratoire d'Electrochimie Analytique et Appliquée, Ecole Nationale Superieure de Chimie de Paris, 11 rue Pierre at Marie Curie, 75231 Paris, cedex 05, France

Y. CASTRILLEJO

Dpto de Quimica Analitica, Facultad de Ciencias Universidad de Valladolid, Prado de la Magdalene s/n, 47005 Valladolid, España

Received 23 December 1991: revised 25 May 1992

The stability of nickel chloride and oxide as well as the electrochemical behaviour of the Ni^{2+} ion have been studied in $ZnCl_2$–2NaCl melts at 450° C by means of X-ray diffractions (XRD), potentiometry, cyclic voltammetry, chronoamperometry and chronopotentiometry.

The standard potential of the redox couple Ni(II)/Ni(O) and solubility product of nickel oxide have been determined (E°Ni(s)/Ni(II) = -1.006 ± 0.001 V (against Cl_2(1 atm)/Cl^-), pKs = 4.8 ± 0.1 in molality scale). These results have allowed the construction of E–pO^{2-} equilibrium diagrams.

Nickel (II) reduction is close to the reversibility according to the scheme:

$$NiCl_2(\text{solvated}) + 2e^- \rightleftharpoons Ni(s) + 2Cl^-$$

with a diffusion coefficient, D_{Ni}, close to $3 \times 10^{-6}\,cm^2\,s^{-1}$.

1. Introduction

For many applications of nickel the purity of the metal is of primary significance. One of the principal methods for production of high purity nickel is electrowinning, whose implementation in molten media implies a previous study of chemical and electrochemical behaviour of the metal. Such studies have been carried out to a much greater extent in molten alkali and alkaline earth chlorides than in any other halide system; the more usual solvents being the eutectic LiCl–KCl, the equimolar mixture of KCl–NaCl, and the $MgCl_2$–KCl and $MgCl_2$–NaCl–KCl mixtures [1] in which only the Ni(II) and Ni(O) oxidation states are known to be stable.

Combes *et al.* [2] reported the solubility product of NiO in NaCl–KCl, Bouteillon *et al.* [3] determined the diffusion coefficient of Ni(II) in LiCl–KCl, and Baimakov and Tomskikh studied the effect of temperature, current density, and Ni(II) concentration on the structure of the nickel metal deposited [4].

The purpose of the present investigation has been the acquisition of the necessary fundamental data to propose a process including both treatment of nickel oxide and subsequent electrowinning of metallic nickel in a single melt.

We report the standard potential of the Ni(II)/Ni couple (by addition of pure solid $NiCl_2$ to the $ZnCl_2$–2NaCl melt) as well as the solubility product of NiO on the molality scale, these allow the construction of E–pO^{2-} equilibrium diagrams. Also, we report on the electrochemical behaviour of nickel ions using voltammetric and pulse techniques.

2. Experimental details

2.1. *Preparation and purification of the melt*

The $ZnCl_2$–2NaCl melt, (analytical grade Merck products) was contained in a 100 cm^3 Pyrex crucible placed in a Pyrex cell. The temperature was maintained constant within ± 2 °C by means of a Taner furnace and a Microcor II Coreci programmable device. The mixture was fused under vacuum, purified by bubbling hydrogen chloride and then kept under a dry argon atmosphere, a procedure used previously [5, 8].

2.2. *Electrochemical apparatus*

The e.m.f. measurements were made with a high impedance voltameter (AOIP VNZ). Cyclic voltammetry and pulse techniques were recorded with a potentiostat–galvanostat PAR EG&G Model 173 controlled by an Apple II computer and using the appropriate software (PAR).

Two tungsten wires (1 mm diameter) were used as working and counter electrodes. The reference electrode consisted of a Pyrex glass tube filled with liquid zinc and covered with molten $ZnCl_2$–2NaCl. A tungsten wire was immersed into the liquid zinc to ensure electrical connection with the reference electrode (Zn(II)/Zn(liq) redox couple).

† Deceased.

0021-891X

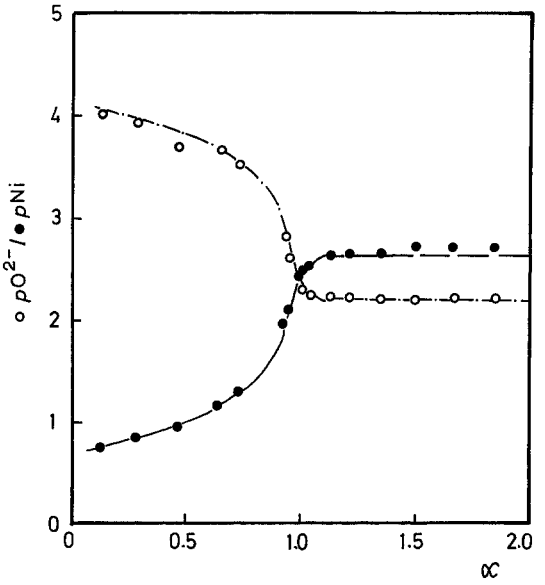

Fig. 1. Potentiometric titration, in molten $ZnCl_2$–2NaCl at 450°C, of nickel chloride 2.06 × 10^{-1} mol kg^{-1} by sodium carbonate. (○) pO^{2-} indicator electrode with yttria-stabilized zirconia membrane; (●) pNi indicator electrode with a nickel wire.

3. Results and discussion

3.1. *Diagram E–pO²⁻ of Ni*

The standard potential of the Ni^{2+}/Ni system was determined by measuring the equilibrium potential of a nickel wire in different solutions containing Ni^{2+} ion concentrations between 6.223 × 10^{-2} and 2.065 × 10^{-1} mol kg^{-1}. A plot of the cell e.m.f. versus the logarithm of the $NiCl_2$ concentration was linear with a slope of 0.070 V (decade)$^{-1}$, in agreement with the theoretical value of 0.072 for a two-electron process at 450°C. We found that $E°$(Ni(II)/Ni) is -1.006 ± 0.001 V against the Cl_2/Cl^- reference system.

The activity coefficient of $NiCl_2$ in the melt was estimated from the standard potential of the Ni^{2+}/Ni couple as follows: the ΔE corresponding to the reaction:

$$Ni + Cl_2(g) \rightleftharpoons NiCl_2 \text{ (dissolved)}$$

is related to the ΔE^* of the reaction between pure compounds:

$$Ni(s) + Cl_2(g) \rightleftharpoons NiCl_2(s)$$

by the equation:

$$\Delta E = \Delta E^* - 2.3RT/2F \log f(NiCl_2)$$

from which the activity coefficient $f(NiCl_2)$ can be deduced. ΔE^* was derived from the literature [6] and ΔE from previously recorded experimental data. It was found that $\log f(NiCl_2)$ is 0.11 at 450 °C.

3.1.1. Titration of nickel chloride by carbonate ion and pKs(NiO) determination. The potential values obtained after successive additions of known amounts of sodium carbonate to solutions of nickel chloride, are plotted in Fig. 1 for an initial concentration C_o of Ni(II) 2.06 × 10^{-1} mol kg^{-1}. The curves show only one equivalence point, for a stoichiometric ratio α = added carbonate/nickel(II) equal to 1. This value indicates that the reaction is:

$$Ni^{2+} + O^{2-} \rightleftharpoons NiO(s)$$

The X-ray analysis of the resulting solid compound recovered at the end of the experiment after dissolution of the melt in water and subsequent filtration has proved the existence of NiO, confirming the above reaction. Beyond the equivalence point there was an excess of carbonate ions which led to ZnO precipitation.

Mass action law equations enable the expression of the theoretical functions $\alpha = f(pO^{2-})$ and $\alpha = f(p\text{Ni})$ corresponding to the performed titration.

Before precipitation of NiO ($\alpha < 1$) these expressions are:

$$p\text{Ni} = -\log\left(\frac{C_o(1-\alpha) + \sqrt{C_o^2(\alpha-1)^2 + 4Ks\text{NiO}}}{2}\right)$$

and

$$p\text{Ni} = pKs\text{NiO} + \log\left(\frac{C_o(1-\alpha) + \sqrt{C_o^2(\alpha-1)^2 + 4Ks\text{NiO}}}{2}\right)$$

When NiO is precipitated ($\alpha > 1$) they become:

$$p\text{Ni} = pKs\text{NiO} - pKs\text{ZnO}$$

and $pO^{2-} = pKs\text{ZnO}$.

In order to obtain the value of Ks(NiO) from the experimental results, a simulation method was used based on these equations giving arbitrary values to the constants. The simulated curve which best fits the experimental data is shown in Fig. 1. The corresponding value of Ks(NiO) is 4.8 ± 0.1.

In order to compare the experimental solubility product with the values calculated from thermodynamic data, the solubility product corresponding to the reaction:

$$Ni^{2+} + O^{2-} \rightleftharpoons NiO$$

was calculated by means of the reaction between the pure compounds

$$ZnO + NiCl_2 \rightleftharpoons NiO + ZnCl_2$$

and the relation

$$pKs(\text{NiO}) = -pK^* - \log a(ZnCl_2) + pKs(\text{ZnO}) + \log f(NiCl_2)$$

pK^* was calculated from the chemical potentials given by Barin *et al.* [6] while $\log a(ZnCl_2)$ and pKsZnO were determined previously [7, 8].

The values so obtained, pKs = 4.75, is in good agreement with the experimental values. All the calculated data were then used to build up the equilibrium potential-acidity diagrams for nickel compounds (Fig. 2).

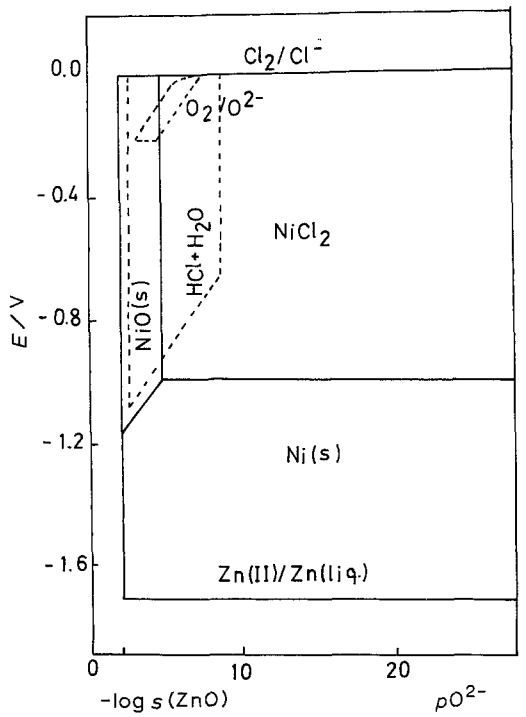

Fig. 2. Equilibrium potential acidity diagram for nickel compounds (solid lines) and the mixtures $Cl_2 + O_2$, $HCl + H_2O$ (dotted lines), for pressures between 1 and 10^{-3} atm, in the melt $ZnCl_2$–2NaCl at 450 °C.

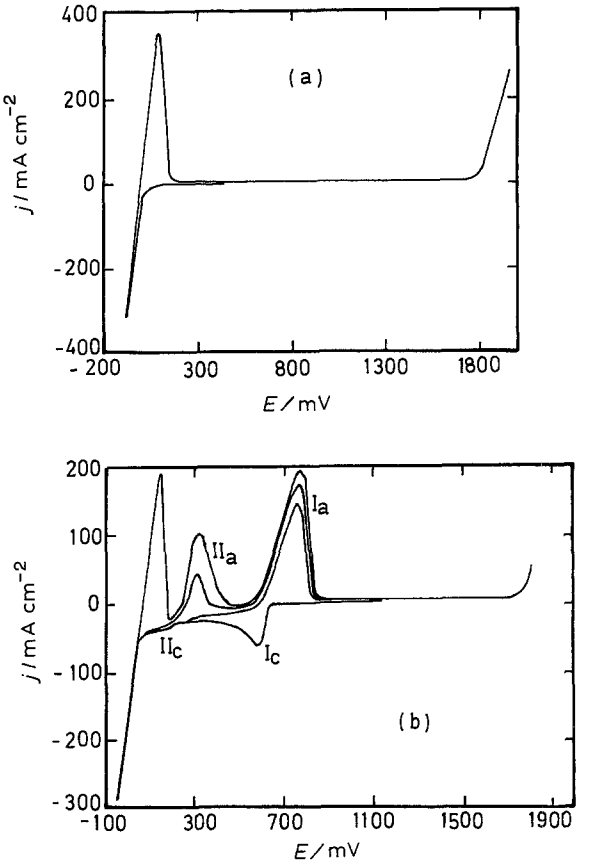

Fig. 3. (a) Cyclic voltammogram obtained at a tungsten electrode ($s = 0.16\,cm^2$) in a pure $ZnCl_2$–2NaCl melt (sweep rate: $0.5\,V\,s^{-1}$). (b) Typical cyclic voltammograms for the reduction of nickel chloride $0.049\,mol\,kg^{-1}$ on a tungsten electrode for different inversion potentials (sweep rate: $0.2\,V\,s^{-1}$).

3.2. *Electrochemical study of Ni deposition*

After the purification of the $ZnCl_2$–2NaCl melt, and using tungsten electrodes, the electrochemical window of the melt was 1.780 V, extending from 1.780 V (chlorine evolution) to 0.000 V (zinc deposition) with respect to the Zn(II)/Zn reference electrode (Fig. 3(a)) [8].

Figure 3b presents a number of voltammograms for the reduction of nickel chloride on a tungsten electrode. On each curve a cathodic peak, I_c, and, on the anodic part of the curve, one sharp anodic stripping peak, I_a, are evident. The shape of the voltammograms, the break corresponding to the beginning of the nickel chloride reduction (characteristic of the formation and the reoxidation of a constant activity product), and the peak potentials values, all confirm the deposition of nickel.

The cathodic wave II_c, associated with the stripping peak II_a expected for more cathodic inversion potentials, could be attributed to the reduction of Zn(II) on to the tungsten electrode coated with Ni(s), originating the formation of a Ni–Zn alloy.

3.2.1. Reversibility of the Ni(II)Ni(s) electrochemical system on a tungsten electrode. Cyclic voltammograms yield more information about the nickel electrodeposition process. The study of the voltammetric curves recorded with potential sweep rates ranging from 0.05 to $1.2\,V\,s^{-1}$ (Fig. 4(a)) clearly shows the linear dependence of the cathodic peak current, I_c, on the square root of the sweep rate (Fig. 4(b)), and it becomes clear that the reduction step consists of a simple diffusion-controlled charge transfer process.

On the other hand, the peak potential only changes slightly with sweep rate and for values lower than $0.4\,V\,s^{-1}$ the slope of the plot of $\log (i_p - i)$ against E, over the approximate current range $0.5i_p - 0.9i_p$ (Fig. 5), approaches the theoretical value of $2.2nF/RT$ corresponding to a reversible system [9]. At higher sweep rates, the slope deviates from the theoretical value.

Another reversibility test consists in computing the semi-integral of the current $m(t) = (1/\pi)^{-1/2} \int_0^t i(u)(t - u)^{-1/2}\,du$. A convoluted curve, $m = f(E)$, is represented in Fig. 6, after correction of the ohmic drop. The logarithmic analysis of a convoluted curve corresponding to a sweep rate of $0.8\,V\,s^{-1}$ is given in the same Fig. 6. The electrode potential varies linearly with $\log [(m^* - m)/m^*]$ with $m^* = nFCSD^{1/2}$ and the slope of the linear part of this curve is 0.068 V, a value that approaches that expected for a reversible exchange process (0.072 V) [10].

A further study of the electrochemical reduction of Ni(II) was made using chronopotentiometry. Fig. 7 (a) gives the typical chronopotentiograms obtained at a tungsten electrode for imposed cathodic current density values ranging from 12.5 to $125.0\,mA\,cm^{-2}$. The analysis of the transition time variation as a function of the imposed current density, j_0, confirms that the electrochemical reaction is diffusion controlled (Sand's law) (Table 1). Under these conditions the logarithmic analysis of chronopotentiograms is possible as shown in Fig. 7(b): the electrode potential

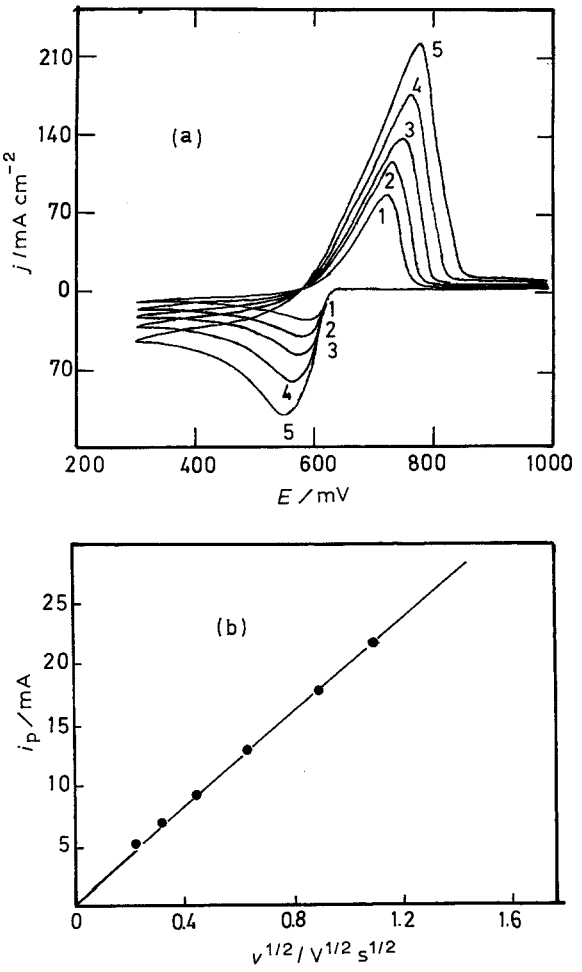

Fig. 4. (a) Voltammetric study of nickel chloride $NiCl_2$ concentration: 0.049 M; sweep rates: (1) 0.05, (2) 0.1, (3) 0.2 (4) 0.4 and (5) 0.8 V s^{-1}. (b) Variation of the cathodic current peak with the square root of the sweep rate at 450 °C.

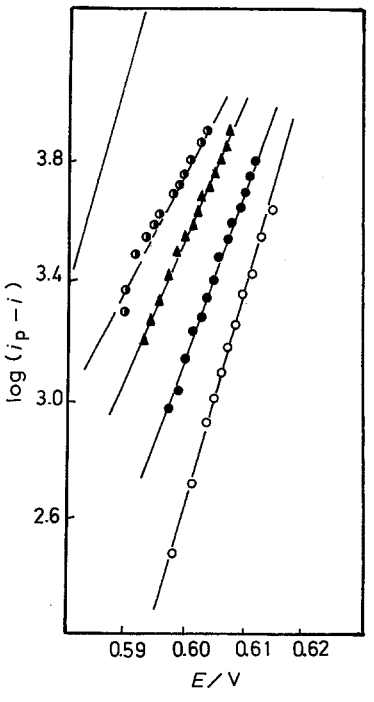

Fig. 5. Plot of log (i_p − i) against E for Ni(II) reduction. (○) 0.2, (●) 0.4, (▲) 0.8 and (◑) 1.2 V s^{-1}; (——) theoretical slope.

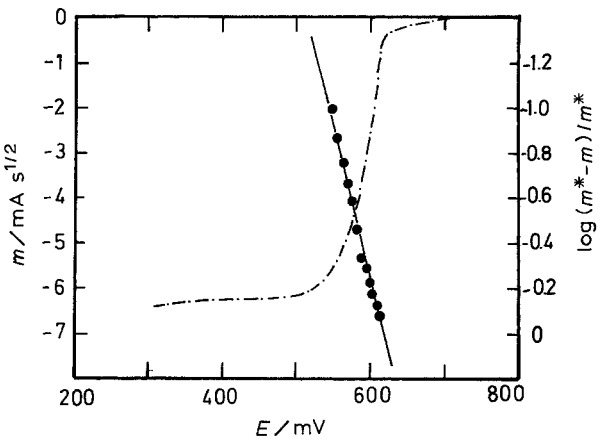

Fig. 6. Semi-integral curve of a voltammogram recorded at 1.2 V s^{-1} (– – –) and its logarithmic analysis (●).

varies linearly with log [1 $-(t/\mathcal{T})^{1/2}$]. The slope of the linear part of the curve (0.065) is close to the theoretical value for a two electron reversible exchange process (0.072) at 450 °C.

All those criteria show that the electrochemical process is close to the reversibility.

By reversing the current at electrolysis time values smaller than the transition time (current reversal chronopotentiometry) it was found that the ratio of t_{ox} (transition time corresponding to the oxidation of the species formed during the electrolysis of duration t_{red}) to t_{red} is close to unity whatever the imposed current. This fact can only be explained by the presence of a strongly adhering deposit of nickel on to the tungsten electrode (Fig. 7(c)).

3.2.2. Study of nickel ion diffusion. The nickel ion diffusion coefficient was computed from chronopotentiometric, voltammetric data and from the boundary semi-integral values according, to the following relations:

$$\frac{i\mathcal{T}^{1/2}}{C} = \frac{nFSD^{1/2}\pi^{1/2}}{2}$$

$$i_p = 0.610(nF)^{3/2} C\, D^{1/2}\, v^{1/2}\, (RT)^{-1/2}$$

$$m^* = nFSCD^{1/2}$$

where C is the bulk concentration of the oxidized species, D the diffusion coefficient, S the electrode surface and $\mathcal{T}$ the transition time. The results are summarized in Table 2.

A further study of the electrochemical reduction of Ni(II) on the tungsten electrode was made using chronoamperometry between E = 650 mV and E = 0 mV. It was observed that chronoamperograms show a current constant due to thermal convection, for time values greater than 2 s (Fig. 8).

By plotting the variation of the current against $1/t^{1/2}$ at the potential corresponding to the diffusion limiting current of the i–E reduction curve, it can be shown that the experimental data obey the Cottrell law

$$id(t) = \frac{nFSD^{1/2}C}{\pi^{1/2}t^{1/2}}$$

From the slope of the straight line obtained the

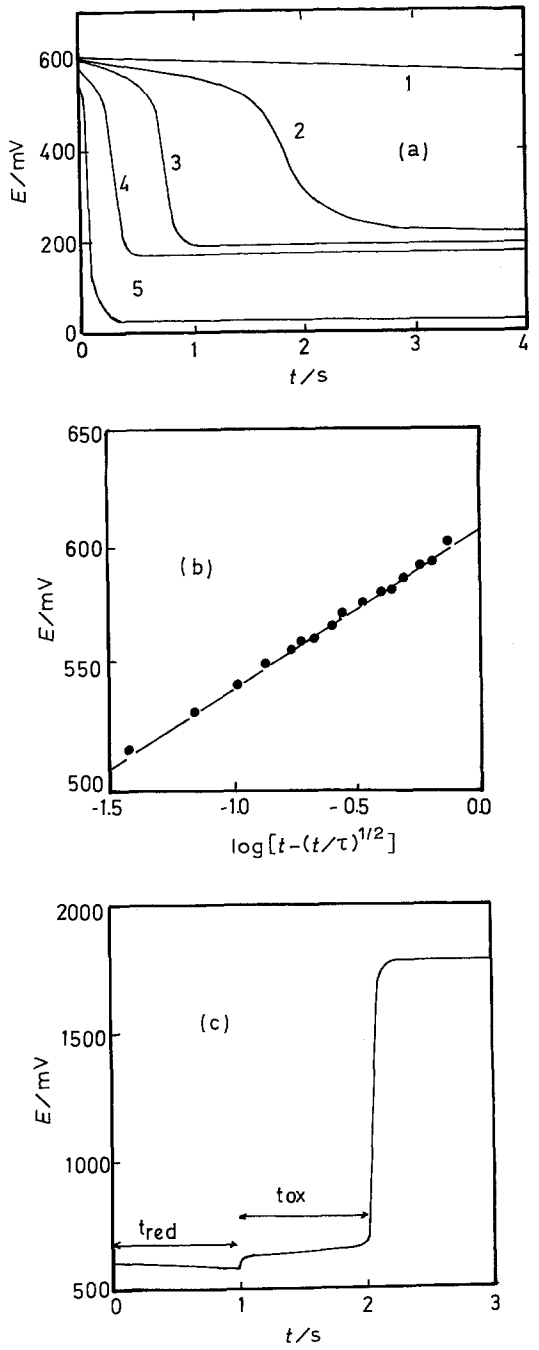

Fig. 7. (a) Chronopotentiometric study of nickel chloride reduction. $NiCl_2$ concentration 0.049 mol kg^{-1}. Cathodic current density (1) 12.5, (2) 21.8, (3) 37.5, (4) 62.5, (5) 125.0 mA cm^{-2}. (b) Logarithmic analysis of chronopotentiograms. Cathodic current density 21.8 mA cm^{-2}. (c) Chronopotentiogram with current reversal j = 21.8 mA cm^{-2}.

Table 1. Chromopotentiometric data for the reduction of $NiCl_2$ 0.049 mol kg^{-1}. *Sand's law verification*

i/mA	$(i^{1/2}/Co)$/As^{-1} mol^{-1} cm^3
−3.5	43
−6.0	48
−9.0	47
−10.0	47
−11.0	45
−12.0	42
−20.0	45

Table 2. Nickel ion diffusion coefficients obtained by different techniques

Technique	$10^6 D_{Ni}$(II)/cm^2 s^{-1}
Voltammetry (semi-integral)	3.7 ± 0.3
Voltammetry ($i_p = f(v^{1/2})$)	3.3 ± 0.5
Chronopotentiometry	2.9 ± 0.4
Chronoamperometry	2.6 ± 0.9

diffusion coefficient D_{Ni} of Ni(II) ion (using a number of exchanged electrons n = 2) was calculated (see Table 2).

4. Conclusions

The chemical properties of nickel in the melt $ZnCl_2$–2NaCl, as well as the mixtures $Cl_2(g)$ + $O_2(g)$ and HCl(g) + H_2O(g), previously determined [5], have been summarized in the form of an equilibrium potential oxoacidity diagram.

The nickel oxide can be chlorinated with the mixture Cl_2 + O_2 for $P(Cl_2)$ = 1 atm and $P(O_2)$ = 10^{-3} atm (quasi-pure chlorine action) and by bubbling HCl containing 1% of water. In the first case, during the chlorinating action, the oxide ions are oxidized to gaseous oxygen, whereas in the second case, oxide ions are transformed into water by action of HCl, according with the following reactions:

$$Cl_2(g) + NiO(s) \rightleftharpoons NiCl_2(\text{dissolved}) + \tfrac{1}{2} O_2(g)$$

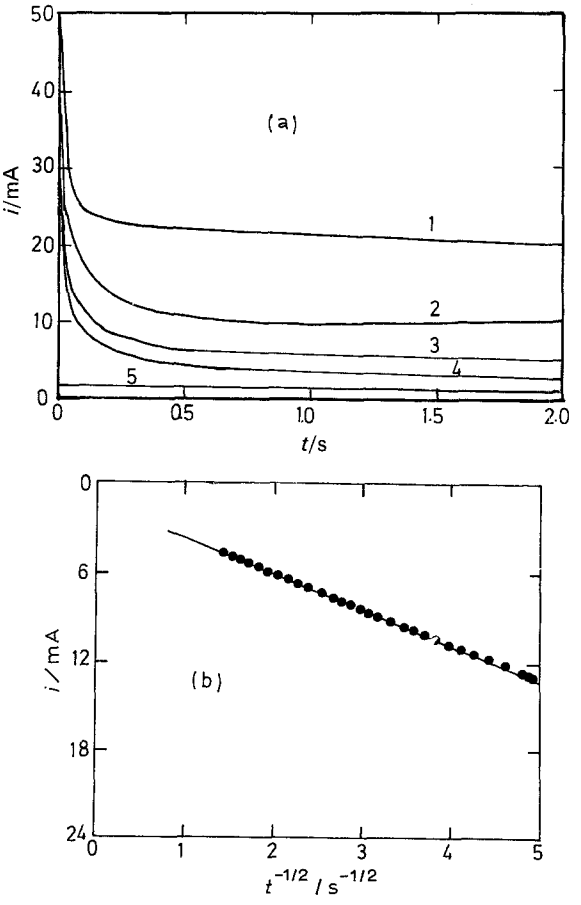

Fig. 8. (a) Chronoamperometric study of nickel chloriode reduction. (b) Verification of Cottrell law.

$$2HCl(g) + NiO(s) \rightleftharpoons NiCl_2(\text{dissolved}) + H_2O(g)$$

The study of the reduction of nickel chloride at a tungsten electrode gives information about the reduction of Ni(II) species, the interaction of nickel with the tungsten electrode and the possibility of formation of Ni–Zn alloys.

Using voltammetric, chronopotentiometric and chronoamperometric techniques the results obtained support a diffusion control for nickel chloride reduction, and it was observed that the electrochemical process is close to the reversibility. The strongly adherence of nickel to the electrode surface and the possibility of formation of an alloy Ni–Zn for more cathodic potentials than the reduction of Ni(II) to Ni(s) has been demonstrated.

Acknowledgements

The authors are grateful to Iberdrola SA (Spain) for financial support for this study.

References

[1] J. A. Plambeck, 'Encyclopedia of Electrochemistry of the Elements' (Fused salt systems), vol 10, (edited by A. J. Bard), Marcel Dekker, New York (1976).
[2] R. Combes, J. Vedel and B. Tremillon, *Anal. Lett.* **3** (1970) 523.
[3] J. Bouteillon and M. J. Barbier, *J. Electroanal. Chem.* **56** (1974) 399.
[4] Yu. V. Baimakov and I. V. Tomskikh, *Electrokhimiya* **2** (1966) 1347.
[5] D. Ferry, Y. Castrillejo and G. Picard, *Electrochim. Acta.* **34** (1989) 313.
[6] Barin and O. Knacke, *in*: 'Thermochemical Properties of Inorganic Substances', Springer, Berlin (1973).
[7] H. Bloom, T. Spurling and J. Wong, *Aust. J. Chem.* **23** (1970) 501.
[8] D. Ferry, Y. Castrillejo and G. Picard, *Electrochim. Acta* **33** (1988) 1661.
[9] G. Mamantov, D. L. Manning and J. M. Dale, *J. Electroanal. Chem.* **9** (1965) 253.
[10] J. C. Imbeaux and J. M. Savéant, *J. Electroanal. Chem.* **44** (1973) 169.
[11] A. J. Bard and L. R. Faulkner, 'Elecrochemical Methods Fundamentals and Applications', John Wiley & Sons, New York (1980).